ISSN: 0067-2904

Designing A Zener Diode Using $Ag_2O_{(1-X)}Zno_{(X)}$/Psi Structures Deposited by Laser Induced Plasma Technique

Raied K. Jamal[*1], Falah Hassen Ali[1], Mohammed M. Hameed[2], Kadhim Abdulwahid Aadim[1]

[1] Physic Department of Physic, College of Science, University of Baghdad, Iraq
[2] Ministry of Higher Education and Scientific Research

Received: 28/10/ 2019 Accepted: 15/3/2020

Abstract

In this paper Zener diode was designed by mixing three mixing ratios of $Ag_2O_{(1-x)}ZnO_{(x)}$, where *x* is 0.5, 0.3, and 0.1, that are deposited on a p-type porous silicon using laser induced plasma technique at room temperature (RT). The results of the Zener diode showed a decrease in knee and Zener voltage when the mixing ratio of $Ag_2O_{(1-x)}ZnO_{(x)}$ structure was increased. Nanofilms of 200nm thickness were prepared from pure ZnO and Ag_2O as well as $Ag_2O_{(1-x)}ZnO_{(x)}$ with three maxing ratios and deposited on glass slides at RT to analyze the structure and optical properties. The structures of Ag_2O and $Ag_2O_{(1-x)}ZnO_{(x)}$ showed high absorbance in the visible region with redshift in spectra when the mixing ratio was increased, while ZnO had a high absorbance in the ultraviolet region. It is concluded that when the value of x increases the energy gap value for the $Ag_2O_{(1-x)}ZnO_{(x)}$ structure decreases.

Keywords: ZnO nanostructure, Ag_2O nanostructure, Zener diode, laser induced plasma.

تصميم زنر دايود باستخدام المركب $Ag_2O_{(1-x)}ZnO_{(x)}$/Psi والمرسب بتقنية البلازما المحتثة بالليزر

رائد كامل جمال*[1]، فلاح حسن علي[1]، محمد مجيد حميد[2]، كاظم عبد الواحد عادم[1]

[1]وزارة التعليم العالي والبحث العلمي، جامعة بغداد، كلية العلوم، قسم فيزياء

[2]وزارة التعليم العالي والبحث العلمي، بغداد، العراق

الخلاصة

في هذه البحث ، تم تصميم الصمام الثنائي نوع زنر من خلال خلط ثلاث نسب مختلفة من(1−x) Ag2O (x) ZnO حيث x هي 0.5 ، 0.3 ، و 0.1 التي رسبت على السيليكون المسامي من النوع p باستخدام تقنية البلازما المستحثة بالليزر في درجة حرارة الغرفة. تُظهر نتائج الصمام الثنائي زنر انخفاضًا في جهد الركبة وجهد زينر عند زيادة الحد الأقصى لنسبة (1−x) AgnO (x) ZnO . تم ترسيب ZnO النقي و Ag_2Oو $Ag2O_{(1-x)}$ $ZnO_{(x)}$ مع ثلاث نسب مختلفة من النانوفيلم بسمك 200 على شريحة زجاجية في درجة حرارة الغرفة لتحليل البنية والخصائص البصرية. أظهر هيكل Ag_2O و $Ag2O_{(1-x)}ZnO_{(x)}$ امتصاصية عالية في المنطقة المرئية مع انزياح أحمر في الأطياف عند زيادة نسبة الخلط، في حين أن ZnO تتمتع بامتصاص عالي في منطقة الأشعة فوق البنفسجية. من خلال النتائج عندما تزيد قيمة x فان قيمة فجوة الطاقة للبنية$Ag2O_{(1-x)}ZnO_{(x)}$ سوف تقل.

*Email: raiedkamel@yahoo.com,

Introduction

ZnO is a semiconductor material that has numerous applications because of its direct and high energy gap (equal to 3.3 eV) near to the UV region [1-5]. ZnO has plentiful opto-electronic applications in solar cells, spintronics [6-10], and laser diodes (LDs) [11]. It is an n-type semiconductor material due to its inner structural flaws such as oxygen and zinc spaces or interstitial situations in the lattice [12]. Ag_2O is a p-type semiconductor with a bandgap of about 1.3 eV. Ag_2O is a tiny dark brown powder used to initialize other silver compounds [13-15].

Numerous mechanisms were utilized to manufacture nanostructured thin films from ZnO/Ag_2O, such as thermal evaporation [16]and sputtering [17], while the laser induced plasma (LIP) is considered as one of the most common and attractive techniques [18]. Among the most important advantages of LIP technology is the ease of obtaining homogeneous films with multiple layers and different materials and compounds. Moreover, the films produced by this technology have a homogeneous distribution.

Zener binaries are involved in the manufacturing of most modern electronic circuits and may be considered as one of the basic units in their construction. One of their most prominent uses is to protect the circuitry from overvoltage. In this paper, a Zener diode was designed by mixing three mixing ratios of $\mathbf{Ag_2O_{(1-x)}ZnO_{(x)}}$, where x has value of 0.5, 0.3, and 0.1, that is deposited on a p-type of porous silicon using laser induced plasma technique at RT.

Experimental details

In this study, ZnO and Ag_2O nanopowders with a purity of 99.99% with three mixing ratios (x=0.5, 0.3, and 0.1) were pressed as a tablet using piston. The ZnO and Ag_2O mixture tablets were 2cm in diameter and 1cm in thickness. Glass substrates of 2.5x7.5 cm^2 were cleaned by an ultrasonic device using water for 10min and then acetone for 10min, followed by drying out in an oven. Pure ZnO, pure Ag_2O, and $\mathbf{Ag_2O_{(1-x)}ZnO_{(x)}}$ nanofilms were precipitated on glass slides using LIP technique at RT, as shown in Figure-1. The LIP deposition parameters maintained for the preparation of all films are given in table 1. To determine the thickness of the prepared films, the optical interferometer method was used. The thickness of each of the pure ZnO, pure Ag_2O, and $\mathbf{Ag_2O_{(1-x)}ZnO_{(x)}}$ films was 200nm. The structural properties of all nanofilms were examined using X-ray diffraction system, while their optical properties were examined using UV/ Visible SP-8001 spectrophotometer.

The Zener diode was designed after deposition of $\mathbf{Ag_2O_{(1-x)}ZnO_{(x)}}$ on the p-type porous silicon which was prepared after leaving the silicon wafer in hydrofluoric acid (HF) for 20 min. The schematic diagram of p-n structure (Zener diode) is shown in Figure-2.

The electrical measurements for the heterojunctions, including the current-voltage characteristic measurements, are shown in Figure-3 at both states of forward and reversed bias.

Results and discussion

The XRD patterns of pure ZnO, pure Ag_2O, and $\mathbf{Ag_2O_{(1-x)}ZnO_{(x)}}$ nanofilms at x=0.5 and RT showed polycrystalline structure, as shown in Fig.(4). Table (2) demonstrates the five strongest peaks with fixing diffraction angle values, FWHM, grain size, and Meller's indices of the prepared nanofilms. The grain size of the crystal structure can be calculated using Scherr's equation [19]:

$$\tau = \frac{K\lambda}{\beta \cos\theta} \quad (1)$$

where (K) is a shape factor that is close to unity, (λ) is the X-ray wavelength, β is the line broadening of full width at half the maximum intensity (FWHM) in radians, and θ is the Bragg angle. The sharp peaks of100, 002, and 101 demonstrated the hexagonal-wurtzite structure of ZnO, while the peaks at 111 and 200 represented the cubic structure of Ag_2O. Fig(4) shows the x-ray diffraction of $\mathbf{Ag_2O_{(1-x)}ZnO_{(x)}}$ structure, where a set of strong diffraction pecks of two materials (coexisting composites) appears.

Figure-5 shows the absorbance spectra as a function of wavelength of pure ZnO, pure Ag_2O, and $\mathbf{Ag_2O_{(1-x)}ZnO_{(x)}}$ nanofilms with three mixing ratios, deposited on glass substrate using laser induced plasma at RT, where negligible scattering is assumed. It can be noticed from this figure that the absorbance spectra were generally high in the ultraviolet regions at 200nm for pure ZnO, 344nm for Ag_2O, and 385nm **for the mixed** $\mathbf{Ag_2O_{(1-x)}ZnO_{(x)}}$ structure. The red shift behavior occurred when the mixing ratio (x) increased. The optical absorption coefficient (α) was calculated as follows [20]:

$$\alpha = 2.303\, A\text{bsorbance} / \textit{thickness of film} \quad (2)$$

The thickness of the prepared nanofilms was 200nm. The absorption spectrum increases with increasing the mixing ratio *x*, leading to increased ZnO crystals, which absorb photon energy.
The $(\alpha h\upsilon)^2$ as a function of photon energy for all nanofilms is shown in Figure-6. The variation of $(\alpha h\upsilon)^2$ is estimated by the Tauc's Equation[21]:

$$(\alpha h\upsilon) = A\,(h\upsilon - E_g)^n \quad (3)$$

where α is the absorption coefficient, A is a constant, $(h\nu)$ is the incident photon energy, and (E_g) is the optical energy bandgap. This equation used a value of n=1/2 for direct transition [8]. The extrapolation of the linear part of the plot $(ah\nu)^2 = 0$, which gives rise to the estimation of the E_g value of all prepared nanofilms. Table-3 shows the E_g values of all prepared samples, where the E_g was decreasing with increasing the mixing ratio *x*, which indicates obtaining a redshift.

Figure-7 reveals that the *n* value was increased with increasing the wavelength of the pure ZnO at a range from 200 nm to 380nm, whereas it was fixed at 2.4 approximately after that. While the *n* value of the pure Ag_2O was increased after 460 nm with increasing the wavelength to 600nm and then fixed at around 2.6. The refractive index spectra of $\mathbf{Ag_2O_{(1-x)}ZnO_{(x)}}$ structure decreased with the increase in *x* (see table 3).

The real part of the dielectric constant value depends on the refractive index (*n*) and the extinction coefficient (*K*), as in the equation below [22]:

$$\varepsilon_r = n^2 - k^2 \quad (4)$$

but the imaginary part depends on the refractive index (*n*) only.

$$\varepsilon i = 2nk \quad (5)$$

where (ε_r) is the real part and (εi) is the imaginary part of the dielectric constant. The spectrum of the excited electron can be explained by the dielectric constant (real and imaginary parts), where the imaginary part represents the absorption of energy from the electric field because of the molecules that possess the bipolar moment in the material, whereas the real part represents the low speed of light in the material.

Figures-(8 and 9) show the spectra of real and imaginary parts of the dielectric constant of all nanofilms. A Zener diode is a type of diode that allows the current to flow in the conventional manner from its anode to its cathode, i.e. when the anode is positive with respect to the cathode. When the voltage across the terminals is reversed and the potential reaches the *Zener voltage* (or "knee"), the junction will breakdown and the current will flow in the reverse direction, which is a desired characteristic. By connecting the electronic circuit as in Fig(3) and plotting the current-voltage characteristic, Fig(10) was obtained. In Fig (10), the greater the value of *x*, the knee voltage or the Zener voltage will decrease, i.e. the relationship between them is inverse.

When looking at the circuit for the Zener diode in the reverse bias case, the voltage in a certain area is almost constant with the flow current. This area is called the breakdown region and the voltage in this region is called the breakdown voltage. But in the forward bias case, the diode acts as a normal diode. Also note that the diode will not work until it reaches a certain voltage value beyond the threshold.

Conclusions

The XRD profiles confirm that the composite is composed of a cubic-phase Ag_2O and a wurtzite-phase ZnO. The activity dependence of the component revealed that the increased value of Ag2O deposited on the composite greatly enhanced the photocatalytic activity. This can be attributed to the notion that the p-n junction in the composite effectively inhibited the recombination of electron–hole pairs.

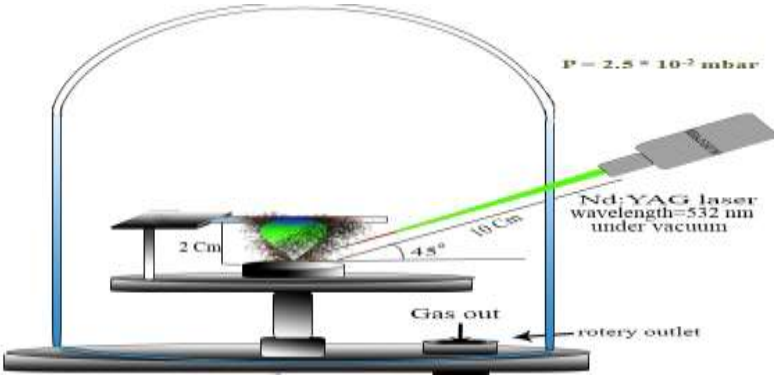

Figure 1-Schematic diagram of LIP technique with λ =532 nm.

Table 1-LIP parameters fixed for the deposited $\mathbf{Ag_2O_{(1-x)}ZnO_{(x)}}$ nanofilms.

Deposition technique	LIP
Deposition target	$\mathbf{Ag_2O_{(1-x)}ZnO_{(x)}}$ where x=0.5, 0.3, and 0.1
Target to substrate distance	2 cm
Chamber pressure	2×10^{-2} mbar
Substrate temperature	301K
Wavelength of laser source	532 nm
Energy of pulse laser	700 mJ
NO. of laser pulse	300

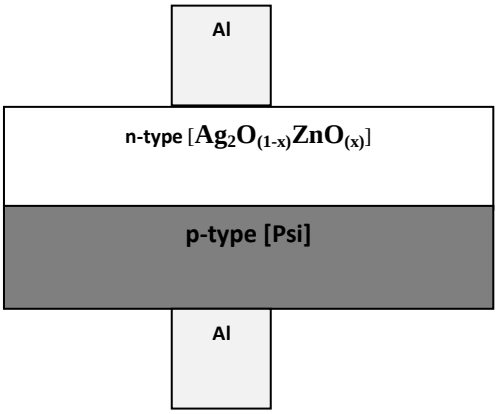

Figure 2-Schematic diagram of the pn structure (Zener diode).

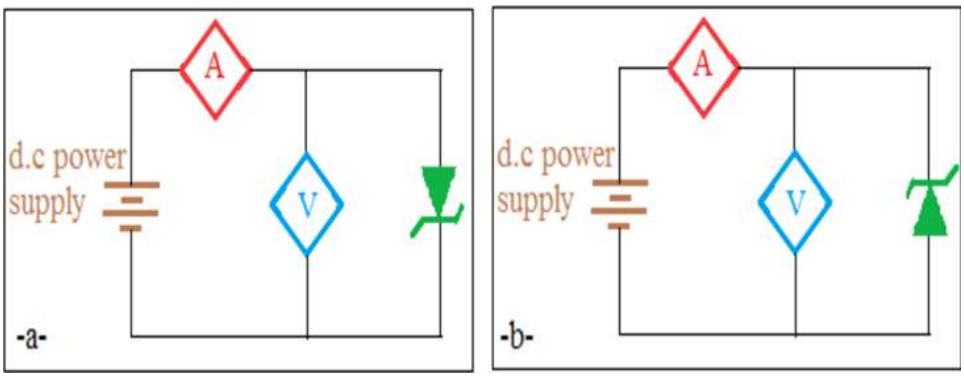

Figure 3-The circuit for I-V measurements for heterojunction. (a) Forward, (b) Reverse bias.

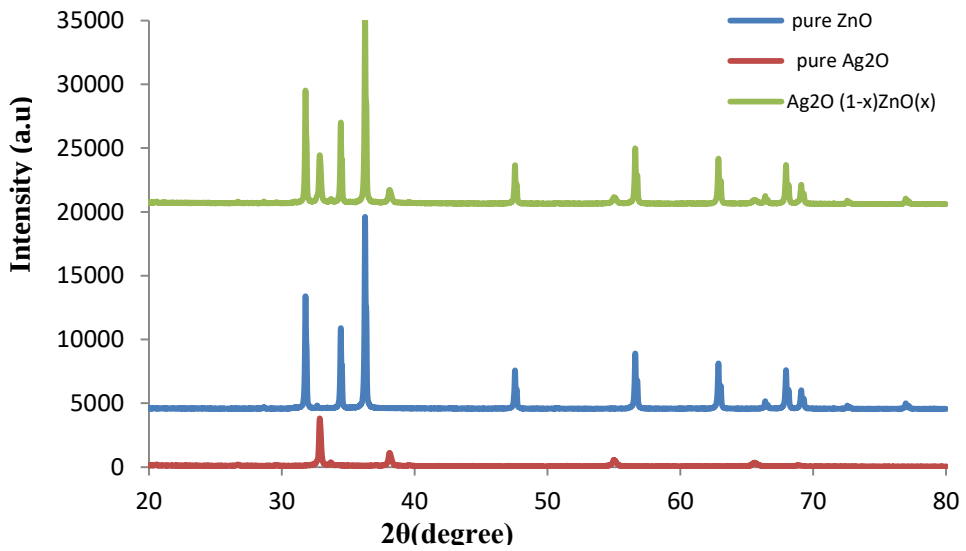

Figure 4-XRD patterns of pure ZnO, pure Ag2O and $\mathbf{Ag_2O_{(1-x)}ZnO_{(x)}}$ nanofilms at x=0.5 and RT.

Table 2-The structural parameters like inter-planar spacing, crystallite size and miller of ZnO and Ag_2O at RT

2θ (Deg.)	FWHM (Deg.)	G.S (nm)	hkl	Phase	Card No.
31.7742	0.3323	24.9	(100)	Hex. ZnO	96-901-1663
34.4449	0.3797	21.9	(002)	Hex. ZnO	96-901-1663
36.2659	0.2847	29.4	(101)	Hex. ZnO	96-901-1663
32.8465	0.31	31.6	(111)	Cub. Ag_2O	00-41-1104
38.107	0.452	25.3	(200)	Cub. Ag_2O	00-41-1104

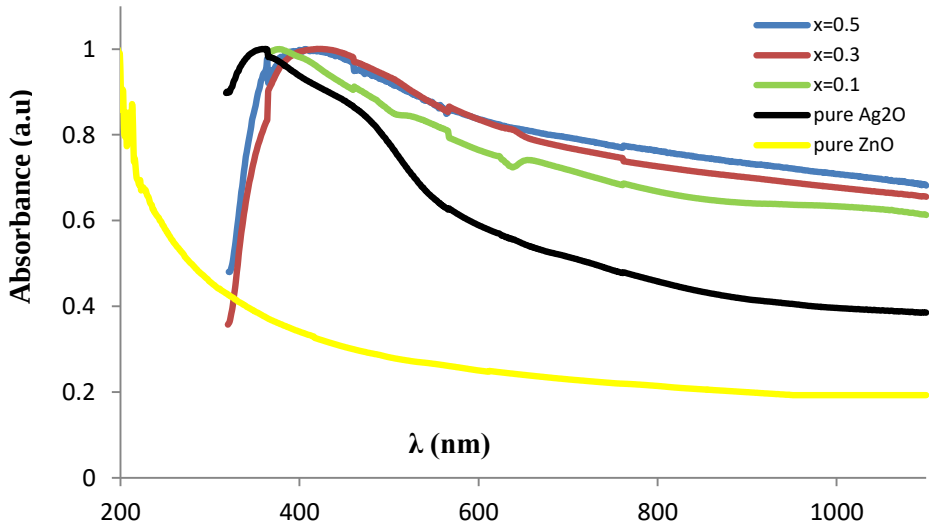

Figure 5-Absorbance spectra of pure ZnO, pure Ag2O and $\mathbf{Ag_2O_{(1-x)}ZnO_{(x)}}$ nanofilms at RT.

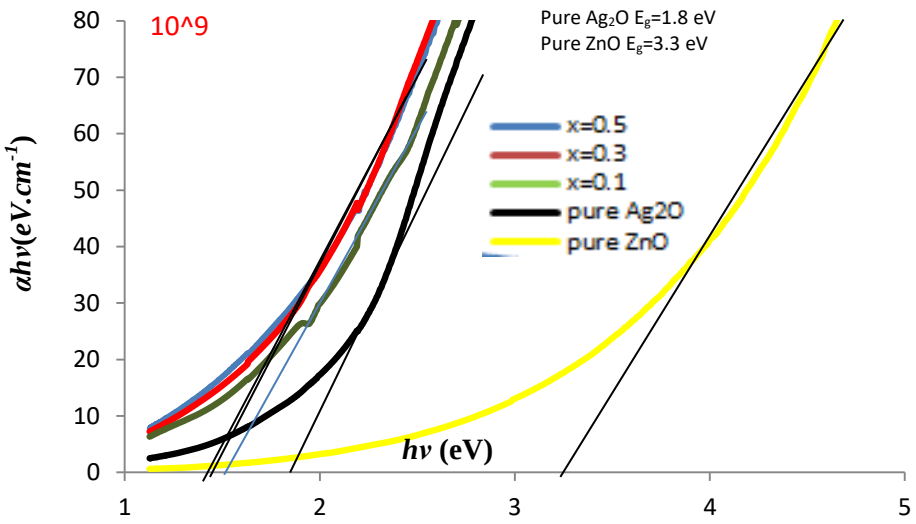

Figure 6-*ahv* spectra of pure ZnO , pure Ag2O and **$Ag_2O_{(1-x)}ZnO_{(x)}$** nanofilms at RT.

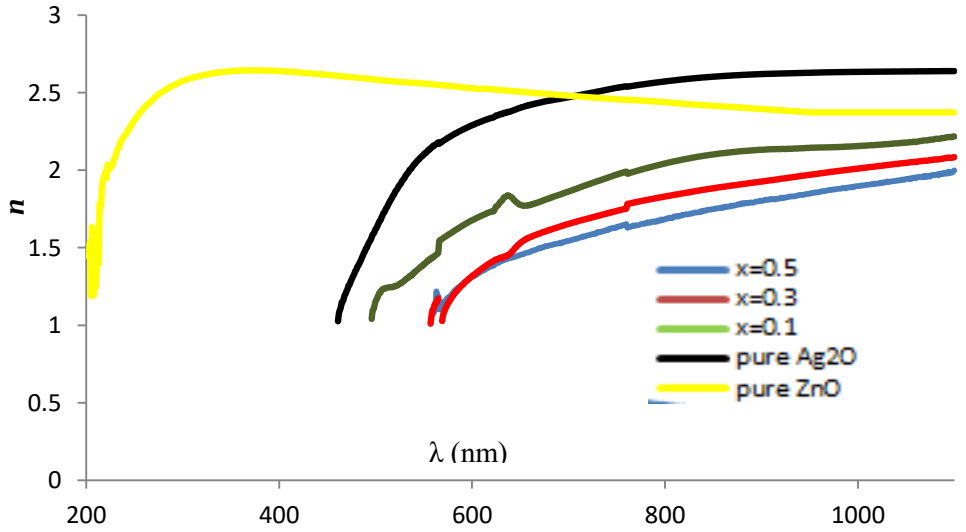

Figure 7-Refractive index spectra of pure ZnO, pure Ag2O and **$Ag_2O_{(1-x)}ZnO_{(x)}$** nanofilms at RT .

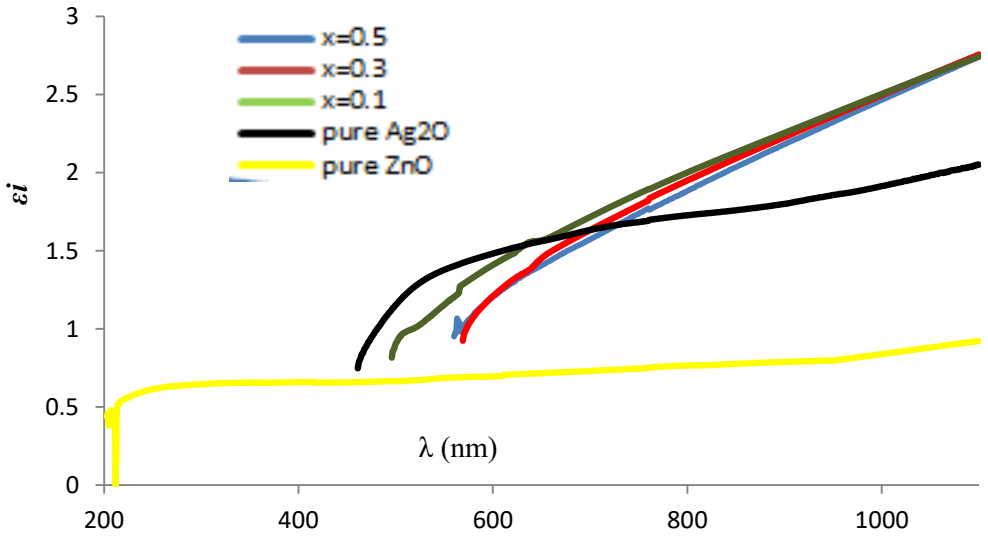

Figure 8- εi spectra of pure ZnO, pure Ag2O and **$Ag_2O_{(1-x)}ZnO_{(x)}$** nanofilms at RT .

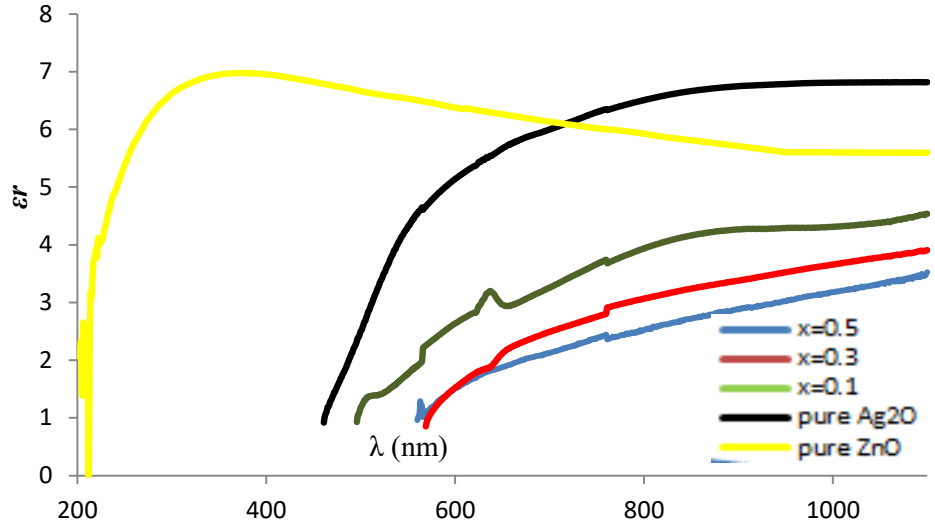

Figure 9-εr spectra of pure ZnO, pure Ag2O and **$Ag_2O_{(1-x)}ZnO_{(x)}$** nanofilms at RT .

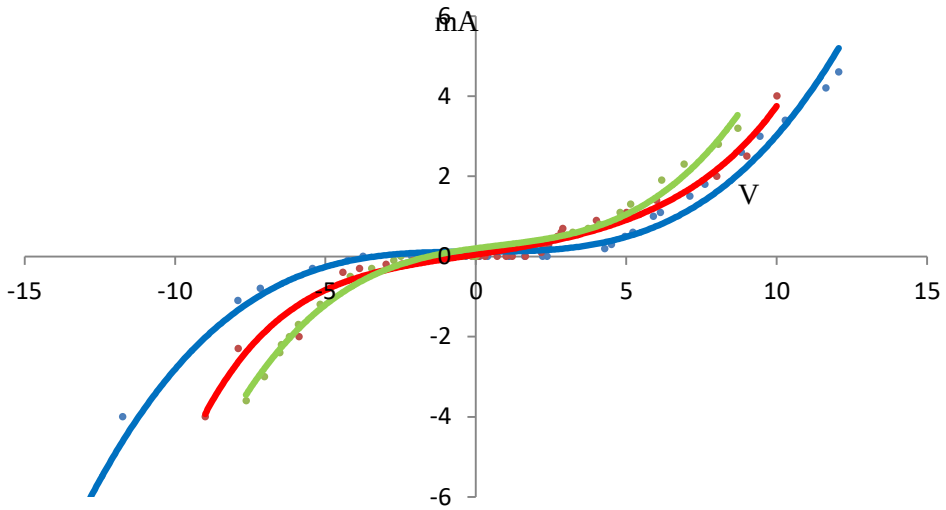

Figure 10- I-V characteristics of Zener diode at(x=0.1-blue line, x=0.3-red line, and x=0.5-green line, at RT.

Table 3-The effect of the mixing ratio (*x*) on Zener and knee voltage and some optical properties at RT.

Structure	Zener voltage(V)	Knee voltage(V)	E_g (eV)	*n at* (vis. and inf.red)region~
Pure ZnO	--	--	3.3	2.44
Pure Ag_2O	--	--	1.87	2.66
x=0.1	13	12.06	1.62	2.1
x=0.3	9	10	1.45	1.99
x=0.5	7.64	8.7	1.44	1.96

References

1. Kowsari E. **2011**. Sonochemically assisted synthesis and application of hollow spheres, hollow prism, and coralline-like ZnO nanophotocatalyst. *J Nanoparticle Res*, **13**: 3363–3376.

2. Mang A, Reimann K and Rubenacke St. **1995**. Band gap, crystal-field splitting, spin-orbit coupling, and exciton binding energies in ZnO under hydrostatic pressure. *Solid State Commun*. **94**(4): 251.

3. Reynolds D C, Look D C, Jogai B, Litton C W, Cantwell G and Harsch W C. **1999**. Valnced-band ordering in ZnO. *Phys. Rev. B*. **60**: 2340.

4. Chen Y, Bagnall D, Koh H, Park K, Hiraga K, Zhu Z. and Yao T. **1998**. Plasma assisted molecular beam epitaxy of ZnO on *c* -plane sapphire: Growth and characterization. *J. Appl. Phys*. **84**: 3912.

5. Raied K. Jamal, Mohammed A Hammed, Kadhim A, Adem.**2014**. Optical properties of nanostructured ZnO prepared by a pulsed laser deposition technique. *Material letters*, **133**: 31-33**.**

6. Look D. **2001**. Recent advances in ZnO materials and devices. *Mater. Sci. Eng. B*. **80**: 383.

7. Ozgur U, Alivov Y, Liu C, Teke A, Reshchikov M, Dogan S, Avrutin V, Cho S. and Morkoc H. **2005**. A compernensive review of ZnO materials and devices. *J. Appl. Phys*. **98**: 041301.

8. Ogale S. **2005**. *Thin Films and Hetero structures for Oxide Electronics*. New York: Springer. E-book.

9. Nickel N. and Terukov E. **2005**. *Zinc Oxide A Material for Micro- and Optoelectronic Applications*. Netherlands: Springer. E-book.

10. Jagadish C and Pearton S. **2006**. *Zinc Oxide Bulk, Thin Films, and Nanostructures*. New York: Elsevier**.** E-book.

11. Sunayna B., Mohammad S, Muhammad M, Fan G and Jianlin L. **2016**. An Sb-doped p-type ZnO nanowire based random laser diode. *IOP nanotechnology*, **27**(6).

12. Reynolds D, Look D. and Jogai B. **1996**. Optically pumped ultraviolet lasing from ZnO. *Solid State Commun*. **99**(12): 873.

13. Holleman, A. F.; Wiberg, E. **2001**. Inorganic Chemistry. Academic Press: San Diego. E-book.

14. Safa K. Mustafa, Raied K. Jamal. **2019**. Studying the Effect of Annealing on Optical and Structure Properties of Zno Nanostructure Prepared by Laser Induced Plasma. *Iraqi Journal of Science*. **60**, (10): 2168.

15. Mundher.A.Hassan.**2012**.Preparation and characterization ZnO nanoparticles and study of morphology at high temperature. *Iraqi Journal of Science*. **10**(18): 17-23.

16. Sze M. **2012**. *Semiconductor Devices: Physics and Technology*. 2end Edition.

17. Windischman, H. **1992**. Intrinsic stress in sputter-deposited thin film. *Crit. Rev. Sol. St.Mat.Sci*. **17**(6): 547-596.

18. Douglas B. Chrisey and Graham K.**1994**. *Pulsed laser deposition of thin films*. edited by John Wiley & Sons.

19. Muniz F, Miranda M, Morilla D, Sasaki J. **2016**. The Scherrer equation and the dynamical theory of X-ray diffraction. *Acta Crystallogr A Found Adv*. **1**: 385.

20. Goetzberger, A.**1998**. *Crystalline Silicon Solar Cells. Chichester*: John Wiley & Sons Ltd.

21. Tauc, J. **1968**. Optical properties and electronic structure of amorphous Ge and Si. *Materials Research Bulletin*. **3**: 37–46.

22. Vikass M. **1997**. IEEE Standard Definitions of Terms for Radio Wave Propagation. IEEE Standards Board.